Proceedings of the ASME 2022 41st International & Conference on Ocean, Offshore and Arctic Engineering
OMAE2022
June 5-10, 2022, Hamburg, Germany

OMAE2022-79230

MODELLING AERODYNAMICS OF A FLOATING OFFSHORE WIND TURBINE USING THE OVERSET MESH SOLVER IN OPENFOAM

Zaibin Lin
Department of Computing and Mathematics
Manchester Metropolitan University
Manchester M1 5GD, United Kingdom
Email: z.lin@mmu.ac.uk

Ling Qian*
Department of Computing and Mathematics
Manchester Metropolitan University
Manchester M1 5GD, United Kingdom
Email: l.qian@mmu.ac.uk

Michele Sergio Campobasso
Department of Engineering
Lancaster University
Lancaster LA1 4YW, United Kingdom
Email: m.s.campobasso@lancaster.ac.uk

Wei Bai
Department of Computing and Mathematics
Manchester Metropolitan University
Manchester M1 5GD, United Kingdom
Email: w.bai@mmu.ac.uk

Yang Zhou
Department of Computing and Mathematics
Manchester Metropolitan University
Manchester M1 5GD, United Kingdom
Email: z.yang@mmu.ac.uk

Zhihua Ma
Department of Computing and Mathematics
Manchester Metropolitan University
Manchester M1 5GD, United Kingdom
Email: z.ma@mmu.ac.uk

ABSTRACT

An accurate prediction of aerodynamic and hydrodynamic loads on an offshore floating wind turbine plays a critical role in determining its operational stability, fatigue life and survivability, as well as optimising its power control system. Therefore, it is essential to develop an integrated aerodynamics and hydrodynamics model, which is capable of capturing both loading on and dynamic response of an entire offshore wind turbine system with high accuracy and reliability. Prior to developing such an integrated model, aerodynamics and hydrodynamics models need to be systematically examined, individually. In this study, the performance of the overset mesh solver in OpenFOAM for modelling aerodynamics of a floating offshore wind turbine rotor is evaluated. A benchmark test on the rotor of a National Renewable Energy Laboratory (NREL) 5MW turbine, which is designed to be mounted on a semi-submersible platform is performed. The predicted power and thrust for cases of the rotor with its centre fixed and undergoing pitching motion are compared between the overset mesh solver, a frequency-domain Naiver-Stokes Computational Fluid Dynamics code and the open-source Blade Element Momentum theory code.

INTRODUCTION

Increasing demand for clean energy has driven the deployment and installation of floating wind turbines in offshore areas, where the environment conditions become more complex compared to the onshore sites due to the additional external loading from waves, current, and mooring lines. The combined effects of these external loading lead to a more complex operational environments for floating offshore wind turbines.

For the prediction of the operational performance of a floating offshore wind turbine (FOWT), there exist different numerical approaches, ranging from the low-fidelity numerical codes based on the Blade Element Momentum (BEM) theory [1, 2] to high-fidelity numerical models based on blade-resolved Navier-Stokes (NS) equations [3–6]. Although low-fidelity models have been widely used in practical engineering design for the wind tur-

*Address all correspondence to this author.

bines that are mounted on the fixed bottom foundation, it needs to be further calibrated for the FOWT system as additional entrainment velocities could be introduced into the FOWT system due to motion response of FOWT driven by the external loading in the offshore area. Therefore, to improve the accuracy and reduce uncertainties of low-fidelity model for FOWT rotors and to capture unsteady aerodynamics around FOWT rotors, a high-fidelity blade-resolved NS model is highly desirable for both academic research and industrial applications.

For the blade-resolved NS model, there are existing codes that can be used to investigate aerodynamics of a FOWT rotor under normal working conditions, such as COSA code [5,6], Arbitrary Mesh Interface (AMI) in OpenFOAM [7,8], and overset mesh solver in OVERFLOW2 [9]. However, under extreme sea conditions, a FOWT support platform may undergo large translational and rotational motions, which, in turn, leads to a relatively large motion at the tower top. This raises challenges for most numerical models as both dynamic motions of the rotor and its unsteady aerodynamics need to resolved at the same time. On the other hand, overset mesh based solvers, due to their favourable feature in dealing with large amplitude of six degree of freedom motions [10, 11], have the potential to model the complicated flow around FOWT rotors.

Aiming at developing an integrated CFD model for predicting dynamic response and survivability of FOWTs under extreme waves, the recently developed overset mesh solver in OpenFOAM has previously been adopted and tested for predicting wave loading on FOWTs [12]. In this study, the code will be further developed and evaluated for modelling FOWT rotor aerodynamics. Two different test cases have been used for this purpose - one with the rotor centre fixed and the other with it under prescribed pitching motion. In addition, effects of different overset mesh configurations on solution accuracy are evaluated and different Courant–Friedrichs–Lewy (CFL) numbers have been used to find the time converged solutions. The numerical results based on overset mesh solver are compared with those from the FAST and COSA code [6] from Lancaster University. Finally, the conclusions from the work are summarised.

NUMERICAL MODELS

Governing equations

In this study, the incompressible Reynolds-Averaged Navier–Stokes (RANS) equations are adopted as the governing equations for fluid flow and are given as follows:

$$\nabla \cdot \bar{\mathbf{u}} = 0 \tag{1}$$

$$\frac{\partial \bar{\mathbf{u}}}{\partial t} + \nabla \cdot [(\bar{\mathbf{u}} - \bar{\mathbf{u}}_g)\bar{\mathbf{u}}] = -\frac{\nabla \bar{p}}{\rho} + \nabla \cdot [\nu_{eff} \nabla \bar{\mathbf{u}} + (\nabla \bar{\mathbf{u}})^T] \tag{2}$$

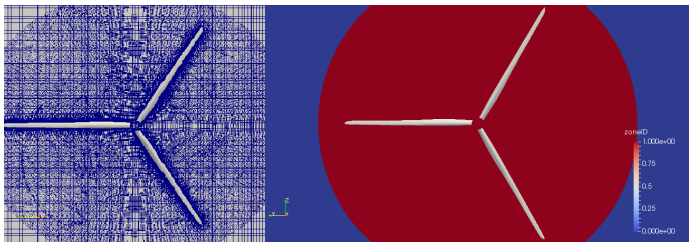

FIGURE 1. MESH SETUPS FOR NUMERICAL MODELS: CIRCULAR DISK FOR ROTOR BLADES.

where $\bar{\mathbf{u}}$ and $\bar{\mathbf{u}}_g$ are the velocity of flow field and grid nodes, respectively; t is the time; $\bar{p}$ is the flow field pressure; ρ is fluid density; $\nu_{eff} = \nu + \nu_t$ is the effective kinematic viscosity of flow, where ν and ν_t are the kinematic and eddy viscosity, respectively.

The shear-stress transport (SST) k-ω turbulence model [13] is used for the closure of the Reynolds term in the equation as it takes the advantages of both k-ω and k-ε turbulence models into consideration, e.g., the boundary layer treatments from k-ω turbulence model and far field treatments from k-ε model. Moreover, the k-ω SST turbulence model has been widely adopted for the simulation of aerodynamics floating offshore wind turbines [4, 7, 8, 14].

Overset mesh method

To overcome the possible mesh distortion induced by the large displacement of a moving structure, the overset mesh solver [15] as developed in OpenFOAM has been extensively used to predict aerodynamics [16] and hydrodynamics [11, 12, 17, 18] around moving structures, which may be difficult to model for the dynamic (moving) mesh approach. For the overset mesh approach, the basic concept is to introduce a composite mesh system with multiple mesh layers, such as a background mesh region and the body-fitted overlapping mesh regions. As a single entity without internal mesh deformation, the body-fitted overlapping mesh regions follow the motion determined by a rigid body motion solver [10, 11]. The data (flow variables) between two types of mesh regions are exchanged via the interpolation at every time step before assembling the matrix.

NUMERICAL SETUPS

To model the flow around a FOWT rotor, two layers of meshes are generated for overset mesh solver in OpenFOAM, one is the background mesh and other other is a smaller overlapping mesh to cover the rotor blades, as highlighted by blue (background) and red (overset) regions respectively in Figs. 1 and 2. In order to examine the effects of overset mesh configurations on the numerical results, two different overset mesh setups, highlighted by red in Figs. 1 and 2, are selected and the overset mesh

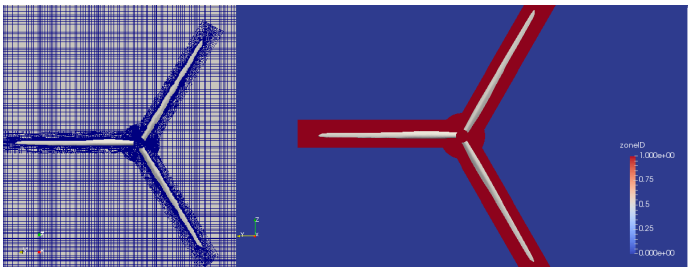

FIGURE 2. MESH SETUPS FOR NUMERICAL MODELS: BODY-FITTED REGION FOR ROTOR BLADES.

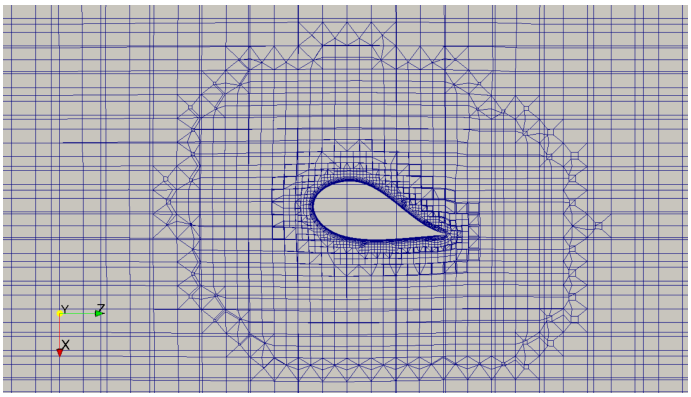

FIGURE 3. BOUNDARY LAYER MESH IN CIRCULAR DISK REGION.

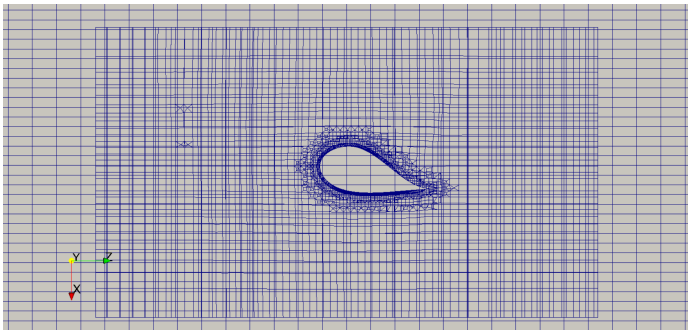

FIGURE 4. BOUNDARY LAYER MESH IN BODY-FITTED REGION.

around the rotor blades is generated using `snappyHexMesh` utility in OpenFOAM. From previous work on modelling wind turbine aerodynamics, it is shown that to capture the turbulent boundary layer flow around the rotor, a sufficiently fine mesh is needed for the region close to rotor blade surfaces. In this work, to maintain a $y+$ value within the required range of 30-600, the boundary layer mesh are generated in the vicinity of the rotor

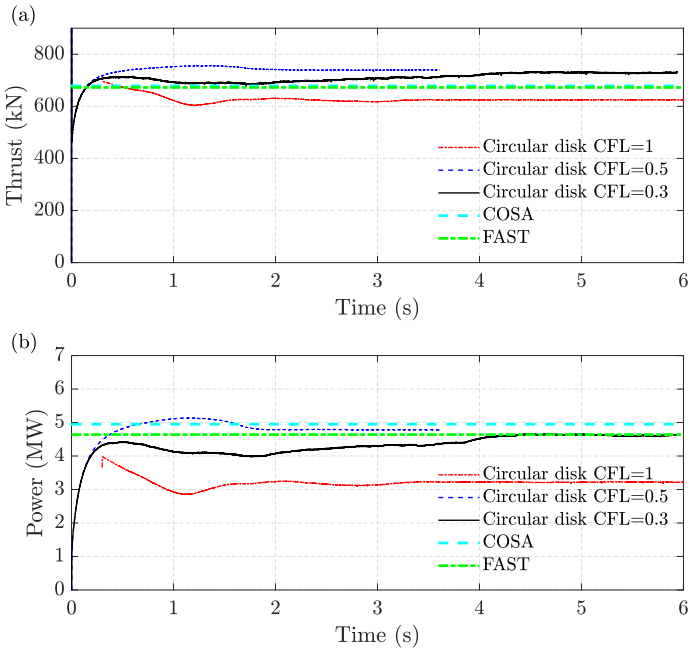

FIGURE 5. COMPARISON OF THRUST AND POWER IN TERMS OF CFL NUMBER CONVERGENCE USING CIRCULAR DISK MESH AGAINST RESULTS FROM FAST AND COSA CODE.

boundaries, where 15 layers of cells are extruded from the rotor boundary surface with a growth rate of 1.1 and first layer thickness of 0.001m. The mesh setups and boundary layer meshes at the cross-sections of the rotor in circular disk and body-fitted regions are presented in Figs. 3 and 4, respectively. The cell numbers for the background mesh and circular disk overset mesh are 2.16 million and 2.44 million, respectively, while they are 7 million and 1.6 million for the background mesh and overset mesh with body-fitted region, respectively.

RESULTS AND DISCUSSIONS

In this section, the numerical results are presented and discussed mainly for the fixed rotor centre case including the effects of the time steps in terms of the Courant–Friedrichs–Lewy (CFL) number on solution convergence and overset mesh configurations. The FOWT rotor used in the present study is the NREL 5 MW virtual turbine. In all the simulations below, a wind speed of 11 m/s and a rotor speed of 12 RPM are adopted. The preliminary results for the case of the rotor undergoing a prescribed pitching motion are also presented.

Effects of CFL numbers

For simulating time-dependent flow problems, the numerical results is highly sensitive to the time step used in the model.

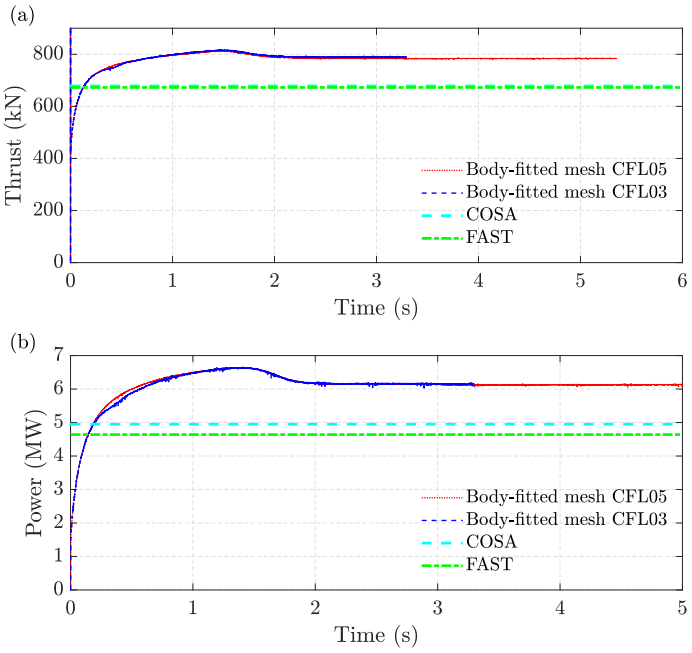

FIGURE 6. COMPARISON OF THRUST AND POWER IN TERMS OF CFL NUMBER CONVERGENCE USING BODY-FITTED MESH AGAINST RESULTS FROM FAST AND COSA CODE.

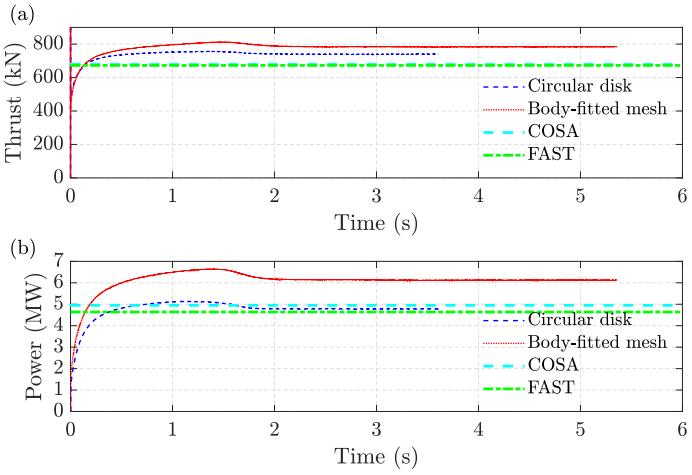

FIGURE 7. COMPARISON OF THRUST AND POWER IN TERMS OF TWO DIFFERENT MESH SETUPS AGAINST RESULTS FROM FAST AND COSA CODE.

The adaptive time step in the present study is determined by the specified maximum CFL number, as shown for a 1D example below:

$$\mathrm{CFL} = \frac{\bar{u}\Delta t}{\Delta x} \leq \mathrm{CFL}_{max} \tag{3}$$

where Δx is a typical cell width. It should be noted that the adaptive time step determined by CFL condition is also related to the mesh grid size and the velocity field. Therefore prior to comparing the effects of overset mesh configurations on the numerical results, the time convergence study is first performed. The CFL numbers selected for the convergence study are 1, 0.5, and 0.3.

In Figs. 5 and 6, the calculated thrust and power with various CFL numbers are presented using two different overset mesh regions. For the case using a circular disk overset region, it is indicated in Fig. 5(a) that varying the CFL number has minor effects on the predicted thrust values, while the effects on the power are slightly more significant compared to the numerical results from FAST and COSA codes. For CFL = 0.5 and 0.3, after reaching the steady-state for each solution, the magnitudes of power are similar to each other and close to the numerical results predicted by the FAST and COSA codes. It can therefore be concluded that time convergence has been achieved using CFL = 0.5 with the circular disk mesh setup shown in Fig. 1.

For the case using a body-fitted overset mesh region, two CFL numbers are selected, namely CFL = 0.5 and 0.3, based on the results for the circular disk overset region. In Fig. 6, it is shown that the time convergence has been achieved using both CFL numbers in terms of the predicted thrust and power values. However, both values are over-predicted using the body-fitted overset region, compared to the numerical results from the FAST and COSA codes.

Overset mesh types

Different overset mesh configurations, such as circular disk and smaller body-fitted mesh, may have certain effects on the numerical results as the hole cutting and data interpolation between background and overset mesh may be different.

In Fig. 7, the numerical results based on two different mesh setups are compared using CFL = 0.5. It is clearly shown that the thrust predicted by both meshes are close to numerical results from the FAST and COSA codes. Nevertheless, the power predicted by body-fitted overset mesh is higher than other numerical results while the power predicted by circular disk agrees well with numerical results from the FAST and COSA codes. The source of this discrepancy may result from the data exchange between background mesh and overset mesh as the overset mesh solver interpolates data from background mesh via its cells that are closely located near the overset region boundary [11].

The hole cutting and data interpolation regions for the two overset mesh meshes are presented in Figs. 8 and 9 for the circular disk and the body-fitted overset mesh, respectively, where the

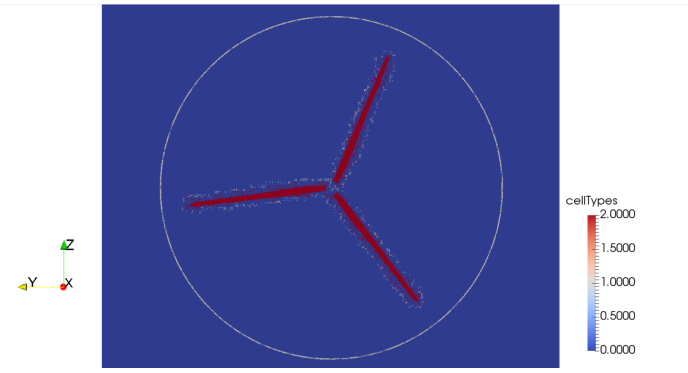

FIGURE 8. HOLE CUTTING AND DATA EXCHANGE FOR CIRCULAR DISK OVERSET MESH SETUP.

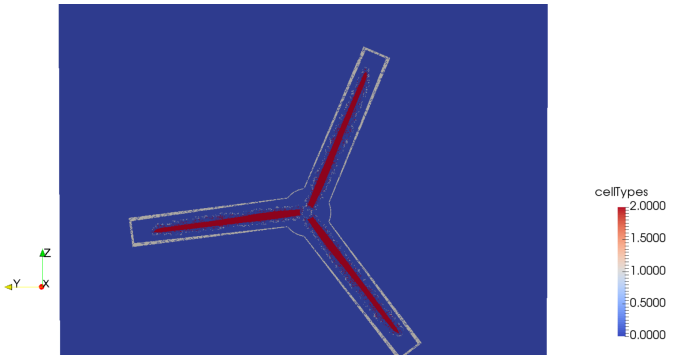

FIGURE 9. HOLE CUTTING AND DATA EXCHANGE FOR BODY-FITTED OVERSET MESH SETUP.

hole cutting is indicated by red colour and the region highlighted by grey colour is used for data interpolation from background mesh to overset mesh. For the body-fitted mesh, the data was interpolated from the fast changing fluid field in the vicinity of rotor surface (see Fig. 11), while for the circular disk mesh the region for data interpolation are far away from the rotor surface where the flow field could be less turbulent (see Fig. 10). The data interpolation at the fast changing flow field may introduce significant numerical errors into the solutions.

Preliminary results on pitching motion

Apart from the numerical results and discussion presented above for the fixed-bottom offshore wind turbine rotor, we also conducted the numerical simulation for the floating offshore wind turbine under pitching motion. The rotor speed and wind speed remain the same as mentioned above, while additional pitching motion is introduced into the rotor motion. The centre of the pitching motion is 90 m vertically below the rotor centre. The prescribed pitching motion is given by the following formula:

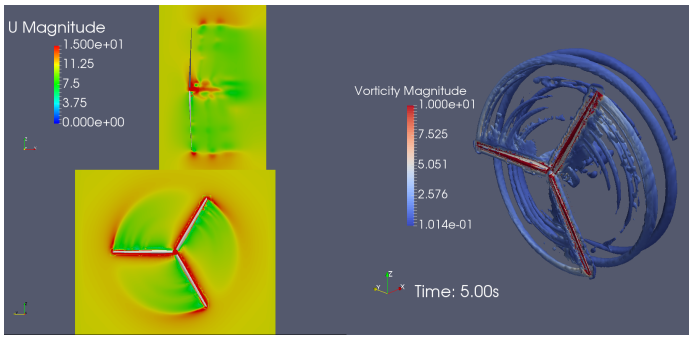

FIGURE 10. VELOCITY FIELD AND VORTEX CONTOUR FOR CIRCULAR DISK OVERSET MESH SETUP.

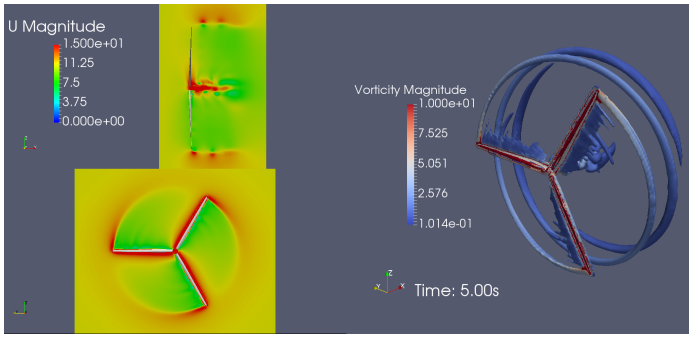

FIGURE 11. VELOCITY FIELD AND VORTEX CONTOUR FOR BODY-FITTED OVERSET MESH SETUP.

$$\theta = \theta_{max} sin(\omega \cdot t) \tag{4}$$

where θ is the time-dependent pitching angle; θ_{max} is the maximum pitching angle and has a value of 1° here; and ω is the angular frequency and equals to 0.62831 rad/s.

Due to the restraint of computational resource, only the preliminary results for this test case are presented in this section. In Fig. 12, the oscillatory thrust and power are plotted for the first 8 seconds of simulation. In contrast to the results for the fixed rotor case in Figs. 5 and 6, the simulation needs to be run for a longer time to reach quasi-steady state solutions. Once this is done, the accuracy of the numerical model under the pitching motion will be further evaluated against experimental measurements and numerical results.

CONCLUSION AND FUTURE WORK

In this study, the performance of the overset mesh solver in OpenFOAM for predicting wind load on FOWT rotors has been

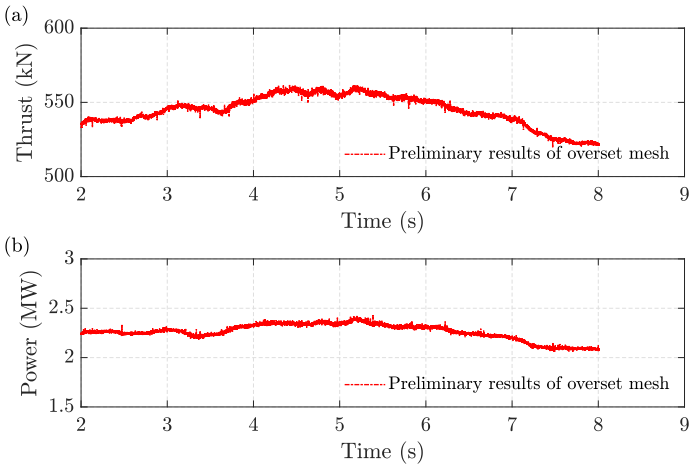

FIGURE 12. THRUST AND POWER OF the ROTOR UNDER PITCHING MOTION.

evaluated. As an example, constant wind flow around an NREL 5 MW wind turbine rotor mounted on a fixed bottom has been simulated and compared with the results from the FAST and COSA codes. Through refining the time steps based on specified CFL numbers, a time step converged solutions can be achieved when CFL = 0.5 for both the overset mesh setups. Effects of different overset mesh configurations on solution accuracy are also investigated. It is found that a larger overset mesh region provides better accuracy as it allows the data exchange between background and overset mesh taking place far away from the turbulent flow field in the proximity of rotor boundary. Currently, the code is being applied to model more complex cases of wind flow around a FOWT rotor undergoing prescribed pitching motions and the results and their validation against available experimental measurements will be presented at the conference.

ACKNOWLEDGMENT

This work was partially funded by the Engineering and Physical Sciences Research Council (EPSRC, UK) projects: Extreme Loading on FOWT under Complex Environmental Conditions (EP/T004150/1), A CCP on Wave Structure Interaction: CCP-WSI (EP/M022382/1) and the Supergen ORE Hub Flexible Fund project: Passive Control of Wave Induced Platform Motions for Semi-submersible FOWTs.

REFERENCES

[1] Coulling, A. J., Goupee, A. J., Robertson, A. N., Jonkman, J. M., and Dagher, H. J., 2013. "Validation of a fast semi-submersible floating wind turbine numerical model with deepcwind test data". *Journal of Renewable and Sustainable Energy,* ***5***(2), p. 023116.

[2] Yang, Y., Bashir, M., Michailides, C., Li, C., and Wang, J., 2020. "Development and application of an aero-hydro-servo-elastic coupling framework for analysis of floating offshore wind turbines". *Renewable Energy,* ***161***, pp. 606–625.

[3] Tran, T.-T., and Kim, D.-H., 2015. "The platform pitching motion of floating offshore wind turbine: A preliminary unsteady aerodynamic analysis". *Journal of Wind Engineering and Industrial Aerodynamics,* ***142***, pp. 65–81.

[4] Tran, T. T., and Kim, D.-H., 2016. "A cfd study into the influence of unsteady aerodynamic interference on wind turbine surge motion". *Renewable Energy,* ***90***, pp. 204–228.

[5] Drofelnik, J., Da Ronch, A., and Campobasso, M. S., 2018. "Harmonic balance navier-stokes aerodynamic analysis of horizontal axis wind turbines in yawed wind". *Wind Energy,* ***21***(7), pp. 515–530.

[6] Ortolani, A., Persico, G., Drofelnik, J., Jackson, A., and Campobasso, M. S., 2020. "Cross-comparative analysis of loads and power of pitching floating offshore wind turbine rotors using frequency-domain navier-stokes cfd and blade element momentum theory". In Journal of Physics: Conference Series, Vol. 1618, IOP Publishing, p. 052016.

[7] Wu, C.-H. K., and Nguyen, V.-T., 2017. "Aerodynamic simulations of offshore floating wind turbine in platform-induced pitching motion". *Wind Energy,* ***20***(5), pp. 835–858.

[8] Liu, Y., Xiao, Q., Incecik, A., and Peyrard, C., 2019. "Aeroelastic analysis of a floating offshore wind turbine in platform-induced surge motion using a fully coupled cfd-mbd method". *Wind Energy,* ***22***(1), pp. 1–20.

[9] Chow, R., and Van Dam, C., 2012. "Verification of computational simulations of the nrel 5 mw rotor with a focus on inboard flow separation". *Wind Energy,* ***15***(8), pp. 967–981.

[10] Ma, Z., Qian, L., Martinez-Ferrer, P., Causon, D., Mingham, C., and Bai, W., 2018. "An overset mesh based multiphase flow solver for water entry problems". *Computers & Fluids,* ***172***, pp. 689–705.

[11] Chen, H., Qian, L., Ma, Z., Bai, W., Li, Y., Causon, D., and Mingham, C., 2019. "Application of an overset mesh based numerical wave tank for modelling realistic free-surface hydrodynamic problems". *Ocean Engineering,* ***176***, pp. 97–117.

[12] Lin, Z., Qian, L., and Bai, W., 2021. "A coupled overset cfd and mooring line model for floating wind turbine hydrodynamics". In The 31st International Ocean and Polar Engineering Conference, OnePetro.

[13] Menter, F. R., Kuntz, M., and Langtry, R., 2003. "Ten years of industrial experience with the sst turbulence model". *Turbulence, heat and mass transfer,* ***4***(1), pp. 625–632.

[14] Leble, V., and Barakos, G., 2016. "Forced pitch motion of wind turbines". In Journal of Physics: Conference Series,

Vol. 753, IOP Publishing, p. 022042.
[15] Hadzic, H., 2006. *Development and application of finite volume method for the computation of flows around moving bodies on unstructured, overlapping grids*. Technische Universität Hamburg.
[16] Tran, T. T., and Kim, D.-H., 2016. "Fully coupled aero-hydrodynamic analysis of a semi-submersible fowt using a dynamic fluid body interaction approach". *Renewable energy,* ***92***, pp. 244–261.
[17] Chen, H., Lin, Z., Qian, L., Ma, Z., and Bai, W., 2020. "Cfd simulation of wave energy converters in focused wave groups using overset mesh". *International Journal of Offshore and Polar Engineering,* ***30***(01), pp. 70–77.
[18] Lin, Z., Chen, H., Qian, L., Ma, Z., Causon, D., and Mingham, C., 2021. "Simulating focused wave impacts on point absorber wave energy converters". *Proceedings of the Institution of Civil Engineers-Engineering and Computational Mechanics,* ***174***(1), pp. 19–31.